

Accelerated Article Preview

Discovering state-of-the-art reinforcement learning algorithms

Received: 11 December 2024

Accepted: 15 October 2025

Accelerated Article Preview



Cite this article as: Oh, J. et al. Discovering state-of-the-art reinforcement learning algorithms. *Nature* <https://doi.org/10.1038/s41586-025-09761-x> (2025)

Junhyuk Oh, Greg Farquhar, Iurii Kemaev, Dan A. Calian, Matteo Hessel, Luisa Zintgraf, Satinder Singh, Hado van Hasselt & David Silver

This is a PDF file of a peer-reviewed paper that has been accepted for publication. Although unedited, the content has been subjected to preliminary formatting. Nature is providing this early version of the typeset paper as a service to our authors and readers. The text and figures will undergo copyediting and a proof review before the paper is published in its final form. Please note that during the production process errors may be discovered which could affect the content, and all legal disclaimers apply.

Discovering state-of-the-art reinforcement learning algorithms

Junhyuk Oh*, Greg Farquhar*, Iurii Kemaev*, Dan A. Calian*, Matteo Hessel, Luisa Zintgraf, Satinder Singh, Hado van Hasselt, David Silver

All authors are affiliated with Google DeepMind, London, UK.

**These authors contributed equally to this work.*

Humans and other animals use powerful reinforcement learning (RL) mechanisms that have been discovered by evolution over many generations of trial and error. By contrast, artificial agents typically learn using hand-crafted learning rules. Despite decades of interest, the goal of autonomously discovering powerful RL algorithms has proven elusive⁷⁻¹². In this work, we show that it is possible for machines to discover a state-of-the-art RL rule that outperforms manually-designed rules. This was achieved by meta-learning from the cumulative experiences of a population of agents across a large number of complex environments. Specifically, our method discovers the RL rule by which the agent's policy and predictions are updated. In our large-scale experiments, the discovered rule surpassed all existing rules on the well-established Atari benchmark and outperformed a number of state-of-the-art RL algorithms on challenging benchmarks that it had not seen during discovery. Our findings suggest that the RL algorithms required for advanced artificial intelligence may soon be automatically discovered from the experiences of agents, rather than manually designed.

The primary goal of artificial intelligence is to design agents that, like humans, can predict and act in complex environments so as to achieve goals. Many of the most successful agents are based on reinforcement learning (RL), in which agents learn by interacting with environments. Decades of research have produced ever more efficient RL algorithms, resulting in numerous landmarks in artificial intelligence including the mastery of complex competitive games such as Go¹, chess², StarCraft³, Minecraft⁴, the invention of new mathematical tools⁵, or the control of complex physical systems⁶.

Unlike humans, whose learning mechanism has been naturally discovered by biological evolution, RL algorithms are typically manually designed. This is usually slow and laborious, and limited by reliance on human knowledge and intuition. Although a number of attempts have been made to automatically discover learning algorithms⁷⁻¹², none have proven to be sufficiently efficient and general to replace hand-designed RL systems.

In this work, we introduce an autonomous method for discovering RL rules solely through the experience of many generations of agents interacting with various environments (Fig. 1a). The discovered RL rule achieves state-of-the-art performance on a variety of challenging RL benchmarks. The success of our method contrasts to prior work in two dimensions. Firstly, while previous methods searched over narrow spaces of RL rules (e.g. hyperparameters^{13,14} or policy loss^{7,12}), our method allows the agent to explore a

36 far more expressive space of potential RL rules. Secondly, while previous work focused on meta-learning
37 in simple environments (e.g. grid-worlds^{9,15}), our method meta-learns in complex and diverse
38 environments at a much larger scale.

39 To choose a general space of discovery, we observe that the essential component of standard RL
40 algorithms is a rule that updates one or more predictions, as well as the policy itself, towards *targets* that
41 are functions of quantities such as future rewards and future predictions. Examples of RL rules based on
42 different targets include temporal-difference learning¹⁶, Q-learning¹⁷, PPO¹⁸, auxiliary tasks¹⁹, successor
43 features²⁰, and distributional RL²¹. In each case, the choice of target determines the nature of the
44 predictions, e.g. whether they become value functions, models, or successor features.

45 In our framework, an RL rule is represented by a *meta-network* that determines the targets towards which
46 the agent should move its predictions and policy (Fig. 1c). This allows the system to discover useful
47 predictions without predefined semantics, as well as how they are used. The system may in principle
48 rediscover past RL rules, but the flexible functional form also allows the agent to invent new RL rules that
49 may be specifically adapted to environments of interest.

50 During the discovery process we instantiate a population of agents, each of which interacts with its own
51 instance of an environment taken from a diverse set of challenging tasks. Each agent's parameters are
52 updated according to the current RL rule. We then use the *meta-gradient* method¹³ to incrementally
53 improve the RL rule such that it could lead to better performing agents.

54 Our large-scale empirical results show that our discovered RL rule, which we call DiscoRL, surpasses all
55 existing RL rules on the environments in which it was meta-learned. Notably, this includes Atari games²²,
56 arguably the most established and informative of RL benchmarks. Furthermore, DiscoRL achieved state-
57 of-the-art performance on a number of other challenging benchmarks, such as ProcGen²³, that it had never
58 been exposed to during discovery. We also show that the performance and generality of DiscoRL
59 improves further as more diverse and complex environments are used in discovery. Finally, our analysis
60 shows that DiscoRL has discovered unique prediction semantics that are distinct from existing RL
61 concepts such as value functions. To the best of our knowledge, this is the empirical evidence that
62 surpassing manually-designed RL algorithms in terms of both generality and efficiency is finally within
63 reach.

64 Discovery Method

65 Our discovery approach involves two types of optimisations: agent optimisation and meta-optimisation.
66 Agent parameters are optimised by updating their policies and predictions towards the targets produced by
67 the RL rule. Meanwhile, the meta-parameters of the RL rule are optimised by updating its targets to
68 maximise the cumulative rewards of the agents.

69 Agent network

70 Much RL research considers what predictions an agent should make (e.g., values), and what loss function
71 should be used to learn those predictions (e.g. TD-learning) and improve the policy (e.g. policy gradient).

72 Instead of hand-crafting them, we define an expressive space of predictions without predefined semantics
73 and meta-learn what the agent needs to optimise by representing it using a meta-network. It is desirable to
74 maintain the ability to represent key ideas in existing RL algorithms, while supporting a large space of
75 novel algorithmic possibilities.

76 To this end we let the agent, parameterised by θ , output two types of predictions in addition to a
77 policy (π): an observation-conditioned vector prediction $y(s) \in \mathbb{R}^n$ and an action-conditioned vector
78 prediction $z(s,a) \in \mathbb{R}^m$ where s and a are an observation and an action (Fig. 1b). The form of these
79 predictions stems from the fundamental distinction between prediction and control¹⁶. For example, value
80 functions are commonly divided into state value functions $v(s)$ (for prediction) and action value
81 functions $q(s,a)$ (for control), and many other concepts in RL, such as rewards and successor features
82 also have an observation-conditioned version $s \vdash \mathbb{R}^m$ and an action-conditioned version $s,a \vdash \mathbb{R}^m$.
83 Therefore, the functional form of the predictions (y,z) is general enough to represent, but is not restricted
84 to, many existing fundamental concepts in RL.

85 In addition to the predictions to be discovered, in most of our experiments the agent makes predictions
86 with pre-defined semantics. Specifically, the agent produces an action-value function $q(s,a)$ and an action-
87 conditional auxiliary policy prediction $p(s,a)$.² This encourages the discovery process to focus on
88 discovering new concepts through y and z .

89 Meta-network

90 A large proportion of modern RL rules use the *forward view* of RL¹⁶. In this view, the RL rule receives a
91 trajectory from timestep t to $t+n$, and uses this information to update the agent's predictions or policy.
92 They typically update the predictions or policy towards *bootstrapped* targets, i.e., towards future
93 predictions.

94 Correspondingly, our RL rule uses a meta-network (Fig. 1c) as a function that determines targets towards
95 which the agent should move its predictions and policy. To produce targets at timestep t , the meta-
96 network receives as input a trajectory of the agent's predictions and policy as well as rewards and episode
97 termination from timestep t to $t+n$. It uses a standard LSTM²⁴ to process these inputs, although other
98 architectures may be used (Extended Data Fig. 3).

99 The choice of inputs and outputs to the meta-network maintains certain desirable properties of
100 handcrafted RL rules. First, the meta-network can deal with any observation, and with discrete action
101 spaces of any size. This is possible because the meta-network does not receive the observation directly as
102 input, but only indirectly via predictions. In addition, it processes action-specific inputs and outputs by
103 sharing weights across action dimensions. As a result it can generalise to radically different environments.
104 Second, the meta-network is agnostic to the design of the agent network, as it only sees the output of the
105 agent network. As long as the agent network produces the required form of outputs (π,y,z), the discovered
106 RL rule can generalise to arbitrary agent architectures or sizes. Third, the search space defined by the
107 meta-network includes the important algorithmic idea of bootstrapping. Fourth, since the meta-network
108 processes both policy and predictions together, it can not only meta-learn auxiliary tasks²⁵ but also

109 directly use predictions to update the policy (e.g., to provide a baseline for variance reduction). Finally,
110 outputting targets is strictly more expressive than outputting a scalar loss function, as it includes semi-
111 gradient methods like Q-learning in the search space. While building on these properties of standard RL
112 algorithms, the rich parametric neural network allows the discovered rule to implement algorithms with
113 potentially much greater efficiency and contextual nuance.

114 Agent optimisation

115 The agent's parameters (θ) are updated to minimise the distance from its predictions and policy to the
116 targets from the meta-network. The agent's loss function can be expressed as:

$$117 \quad L(\theta) = \mathbb{E}_{s,a,s' \sim \pi_\theta} [D(\hat{\pi}, \pi_\theta(s)) + D(\hat{y}, y_\theta(s)) + D(\hat{z}, z_\theta(s, a)) + L_{aux}]$$

118 where $D(p,q)$ is a distance function between p and q . We chose the Kullback–Leibler (KL) divergence as
119 the distance function, as it is sufficiently general and has previously been found to make meta-
120 optimisation easier⁹. Here $\pi_\theta, y_\theta, z_\theta$ and $\hat{\pi}, \hat{y}, \hat{z}$ are the outputs of the agent network and the meta-network,
121 respectively, with a softmax function applied to normalise each vector.

122 The auxiliary loss L_{aux} is used for predictions with pre-defined semantics: action-values (q) and auxiliary
123 policy predictions (p) as follows: $L_{aux}=D(\hat{q},q_\theta(s,a))+D(\hat{p},p_\theta(s,a))$, where \hat{q} is an action-value target from
124 Retrace²⁶ projected to a two-hot vector², and $\hat{p}=\pi_\theta(s')$ is the policy at the one-step future state. To be
125 consistent with the rest of losses, we use the KL divergence as the distance function D .

126 Meta-optimisation

127 Our goal is to discover an RL rule, represented by the meta-network with meta-parameters η , that allows
128 agents to maximise rewards in a variety of training environments. This discovery objective $J(\eta)$ and its
129 *meta-gradient* $\nabla_\eta J(\eta)$ can be expressed as:

$$130 \quad J(\eta) = \mathbb{E}_{\mathcal{E}} \mathbb{E}_\theta [J(\theta)], \quad \nabla_\eta J(\eta) \approx \mathbb{E}_{\mathcal{E}} \mathbb{E}_\theta [\nabla_\eta \theta \nabla_\theta J(\theta)],$$

131 where \mathcal{E} indicates an environment sampled from a distribution, and θ denotes agent parameters induced
132 by an initial parameter distribution and their evolution over the course of learning with the RL rule.
133 $J(\theta)=\mathbb{E}[\sum_t r_t]$ is the expected discounted sum of rewards, which is the typical RL objective. The meta-
134 parameters are optimised using gradient ascent following the above equations.

135 To estimate the meta-gradient, we instantiate a population of agents which learn according to the meta-
136 network in a set of sampled environments. To ensure this approximation is close to the true distribution of
137 interest, we use a large number of complex environments taken from challenging benchmarks, in contrast
138 to prior work that focused on a small number of simple environments. As a result the discovery process
139 surfaces diverse RL challenges, such as the sparsity of rewards, the task horizon, and the partial
140 observability or stochasticity of environments.

141 Each agent's parameters are periodically reset to encourage the update rule to make fast learning progress
142 within a limited agent lifetime. As in prior work on meta-gradient RL¹³, the meta-gradient term $\nabla_{\eta}J(\eta)$
143 can be divided into two gradient terms by the chain rule: $\nabla_{\eta}\theta$ and $\nabla_{\theta}J(\theta)$. The first term can be
144 understood as a gradient over the agent update procedure²⁷, while the second term is the gradient of the
145 standard RL objective. To estimate the first term, we iteratively update the agent multiple times and
146 backpropagate through the entire update procedure as illustrated in Fig. 1d. To make it tractable, we
147 backpropagate over 20 agent updates using a sliding window. Finally, to estimate the second term, we use
148 the advantage actor-critic (A2C) method²⁸. To estimate the advantage, we train a *meta-value* function,
149 which is a value function used only for discovery.

150 Empirical Result

151 We implemented our discovery method with a large population of agents in a set of complex
152 environments. We call the discovered RL rule **DiscoRL**. In evaluation, the aggregated performance was
153 measured by the *interquartile mean* (IQM) of normalised scores for benchmarks that consist of multiple
154 tasks, which has proven to be a statistically reliable metric²⁹.

155 Atari

156 The Atari benchmark²², one of the most studied benchmarks in the history of RL, consists of 57 Atari
157 2600 games. They require complex strategies, planning, and long-term credit assignment, making it non-
158 trivial for AI agents to master. Hundreds of RL algorithms have been evaluated on this benchmark over
159 the last decade, which include MuZero² and Dreamer⁴.

160 To see how strong the rule can be when discovered directly from this benchmark, we meta-trained an RL
161 rule, **Disco57**, and evaluated it on the same 57 games (Fig. 2a). In this evaluation we used a network
162 architecture that has a number of parameters comparable to the number used by MuZero. This is a larger
163 network than the one used during discovery; the discovered RL rule must therefore generalise to this
164 setting. Disco57 achieved an IQM of 13.86, outperforming all existing RL rules^{2,4,14,30} on the Atari
165 benchmark, with a substantially higher wall-clock efficiency compared to the state-of-the-art MuZero
166 (Extended Data Fig. 4) This shows that our method can automatically discover a strong RL rule from such
167 challenging environments.

168 Generalisation

169 We further investigated the generality of Disco57 by evaluating it on a variety of held-out benchmarks
170 that it was never exposed to during discovery. These benchmarks include unseen observation and action
171 spaces, diverse environment dynamics, various reward structures, and unseen agent network architectures.
172 Meta-training hyperparameters were only tuned on training environments (i.e., Atari) to prevent the rule
173 from being implicitly optimised for held-out benchmarks.

174 The result on the ProcGen²³ benchmark (Fig. 2b, Extended Data Table 2), which consists of 16
175 procedurally generated 2D games, shows that Disco57 outperformed all existing published methods,

176 including MuZero² and PPO¹⁸, even though it had never interacted with ProcGen environments during
177 discovery. In addition, Disco57 achieved a competitive performance on Crafter³¹ (Fig. 2d, Extended Data
178 Table 5), where the agent needs to learn a wide spectrum of abilities to survive. Disco57 reached the 3rd
179 place on the leaderboard of NetHack NeurIPS 2021 Challenge³² (Fig. 2e, Extended Data Table 4), where
180 more than 40 teams participated. Unlike the top submitted agents in the competition³³, Disco57 did not
181 use any domain-specific knowledge for defining subtasks or reward shaping. For a fair comparison, we
182 trained an agent with the IMPALA algorithm³⁴ using the same settings as Disco57. IMPALA's
183 performance was much weaker, suggesting that Disco57 has discovered a more efficient RL rule than
184 standard approaches. In addition to environments, Disco57 turned out to be robust to a range of agent-
185 specific settings such as network size, replay ratio, and hyperparameters in evaluation (Extended Data
186 Fig. 1).

187 Complex and diverse environments

188 To understand the importance of complex and diverse environments for discovery, we further scaled up
189 meta-learning with additional environments. Specifically, we discovered another rule, **Disco103**, using a
190 more diverse set of 103 environments consisting of the Atari, ProcGen, and DMLab-30³⁵ benchmarks.
191 This rule performs similarly on the Atari benchmark while improving scores on every other seen and
192 unseen benchmark in Fig. 2. In particular, Disco103 reached human-level performance on Crafter and
193 neared MuZero's state-of-the-art performance on Sokoban³⁶. These results show that the more complex
194 and diverse the set of environments used for discovery, the stronger and more general the discovered rule
195 becomes, even on held-out environments that were not seen during discovery. Discovering Disco103
196 required no changes to the discovery method compared to Disco57 other than the set of environments.
197 This shows that the discovery process itself is robust, scalable, and general.

198 To further investigate the importance of using complex environments, we ran our discovery process on 57
199 grid-world tasks that are extended from prior work⁹, using the same meta-learning settings as for Disco57.
200 The new rule had a significantly worse performance (Fig. 3c) on the Atari benchmark. This verifies our
201 hypothesis about the importance of meta-learning directly from complex and challenging environments.
202 While using such environments was crucial, there was no need for a careful curation of the correct set of
203 environments; we simply used popular benchmarks from the literature.

204 Efficiency and scalability

205 To further understand the scalability and efficiency of our approach, we evaluated multiple Disco57s over
206 the course of discovery (Fig. 3a). The best rule was discovered within approximately 600 million steps
207 per Atari game, which amounts to just 3 experiments across 57 Atari games. This is arguably more
208 efficient than the manual discovery of RL rules, which typically requires many more experiments to be
209 executed, in addition to the time of the human researchers.

210 Furthermore, DiscoRL performed better on the unseen ProcGen benchmark as more Atari games were
211 used for discovery (Fig. 3b), showing that the resulting RL rule scales well with the number and diversity
212 of environments used for discovery. In other words, the performance of the discovered rule is a function
213 of data (i.e., environments) and compute.

214 Effect of discovering new predictions

215 To study the effect of the discovered semantics of predictions (y, z in Fig. 1b), we compared different rules
216 by varying the outputs of the agent, with and without certain types of predictions. The result in Fig. 3c
217 shows that the use of a value function dramatically improves the discovery process, which highlights the
218 importance of this fundamental concept of RL. On the other hand, the result in Fig. 3c also shows the
219 importance of discovering new prediction semantics (y and z) beyond pre-defined predictions. Overall,
220 increasing the scope of discovery compared to prior work⁷⁻¹² was essential. In the following section, we
221 provide further analysis to uncover what semantics have been discovered.

222 **Analysis**

223 **Qualitative analysis**

224 We analysed the nature of the discovered rule, using Disco57 as a case study (Fig. 4). Qualitatively, the
225 discovered predictions spike in advance of salient events such as receiving rewards or changes in the
226 entropy of the policy (Fig. 4a). We also investigated which features of the observation cause the meta-
227 learned predictions to respond strongly, by measuring the gradient norm associated with each part of the
228 observation. The result in Fig. 4b shows that meta-learned predictions tend to pay attention to objects that
229 may be relevant in the future, which is distinct from where the policy and the value function pay attention
230 to. These results indicate that DiscoRL has learned to identify and predict salient events over a modest
231 horizon, and thus complements existing concepts such as the policy and value function.

232 **Information analysis**

233 To confirm the qualitative findings, we further investigated what information is contained in the
234 predictions. We first collected data from the DiscoRL agent on 10 Atari games and trained a neural
235 network to predict quantities of interest from either the discovered predictions, the policy, or the value
236 function. The results in Fig. 4c shows that the discovered predictions contain greater information about
237 upcoming large rewards and the future policy entropy, compared to the policy and value. This suggests
238 that the discovered predictions may capture unique task-relevant information that is not well-captured by
239 the policy and value.

240 **Emergence of bootstrapping**

241 We also found evidence that DiscoRL uses a bootstrapping mechanism. When the meta-network's
242 prediction input at future timesteps (z_{t+k}) is perturbed, it strongly affects the target \hat{z}_t (Fig. 4d). This means
243 that the future predictions are used to construct targets for the current predictions. This bootstrapping
244 mechanism and the discovered predictions turned out to be critical for performance (Fig. 4e). If the y and
245 z inputs to the meta-network are set to zero when computing their targets \hat{y} and \hat{z} (thus preventing
246 bootstrapping), performance degrades substantially. If the y and z inputs are set to zero for computing all
247 targets including the policy target, the performance drops even further. This shows the discovered
248 predictions are heavily used to inform the policy update, rather than just serving as auxiliary tasks.

249 **Previous Work**

250 The idea of meta-learning, or learning-to-learn, in artificial agents dates back to the 1980s³⁷, with
251 proposals to train meta-learning systems with backpropagation of gradients³⁸. The core idea of using a
252 slower meta-learning process to meta-optimize a fast learning or adaptation process^{39,40} has been studied
253 for numerous applications in various contexts, including transfer learning⁴¹, continual learning⁴², multi-
254 task learning⁴³, hyperparameter optimisation⁴⁴, and automated machine learning⁴⁵.

255 Early efforts to use meta-learning for RL agents comprised attempts to meta-learn information-seeking
256 behaviours⁴⁶. Many later works have focused on meta-learning a small number of hyperparameters of an
257 existing RL algorithm^{13,14}. Such approaches have produced promising results but cannot drastically depart
258 from the underlying hand-crafted algorithms. Another line of work has attempted to eschew inductive
259 biases by meta-learning entirely black-box algorithms implemented, for example, as recurrent neural
260 networks⁴⁷ or, as a synaptic learning rule⁴⁸. While conceptually appealing, these methods are prone to
261 overfit to tasks seen in meta-training⁴⁹.

262 The idea of representing knowledge using a wider class of predictions was first introduced in temporal-
263 difference networks⁵⁰ but without any meta-learning mechanism. A similar idea has been explored for
264 meta-learning auxiliary tasks²⁵. Our work extends this idea to effectively discover an entire loss function
265 that the agent optimises, covering a much broader range of possible RL rules. Furthermore, unlike prior
266 work the discovered knowledge can generalise to unseen environments.

267 Recently, there have been growing interests in discovering general-purpose RL rules^{7,9-12,15}. However,
268 most of them were limited to small agents and simple tasks, or the scope of discovery was limited to a
269 partial RL rule. Therefore, their rules were not extensively compared to state-of-the-art rules on
270 challenging benchmarks. In contrast, we search over a larger space of rules, including entirely new
271 predictions, and scale up to a large number of complex environments for discovery. As a result, we
272 demonstrate that it is possible to discover a general-purpose RL rule that outperforms a number of state-
273 of-the-art rules on challenging benchmarks.

274 **Conclusion**

275 Enabling machines to discover learning algorithms for themselves is one of the most promising ideas in
276 artificial intelligence due to its potential for open-ended self-improvement. This work has taken a step
277 towards machine-designed reinforcement learning algorithms that can compete with and even outperform
278 some of the best manually-designed algorithms in challenging environments. We also showed that the
279 discovered rule becomes stronger and more general as it gets exposed to more diverse environments. This
280 suggests that the design of RL algorithms for advanced artificial intelligence may in the future be led by
281 machines that can scale effectively with data and compute.

References

1. Silver, D. et al. Mastering the game of Go with deep neural networks and tree search. *Nature* 529, 484 (2016).
2. Schrittwieser, J. et al. Mastering atari, go, chess and shogi by planning with a learned model. *Nature* 588, 604-609 (2020).
3. Vinyals, O. et al. Grandmaster level in starcraft ii using multi-agent reinforcement learning. *Nature* 575, 350-354 (2019).
4. Hafner, D., Pasukonis, J., Ba, J. & Lillicrap, T. Mastering diverse control tasks through world models. *Nature* (2025).
5. Fawzi, A. et al. Discovering faster matrix multiplication algorithms with reinforcement learning. *Nature* 610, 47-53 (2022).
6. Degraeve, J. et al. Magnetic control of tokamak plasmas through deep reinforcement learning. *Nature* 602, 414-419 (2022).
7. Kirsch, L., van Steenkiste, S. & Schmidhuber, J. Improving generalization in meta reinforcement learning using learned objectives. *International conference on learning representations* (2020).
8. Kirsch, L. et al. Introducing symmetries to black box meta reinforcement learning. *AAAI conference on artificial intelligence* (2022).
9. Oh, J. et al. Discovering reinforcement learning algorithms. *Advances in neural information processing systems* 33 (2020).
10. Xu, Z. et al. Meta-gradient reinforcement learning with an objective discovered online. *Advances in neural information processing systems* 33 (2020).
11. Houthooft, R. et al. Evolved policy gradients. *Advances in neural information processing systems* 31 (2018).
12. Lu, C. et al. Discovered policy optimisation. *Advances in neural information processing systems* (2022).
13. Xu, Z., van Hasselt, H. P. & Silver, D. Meta-gradient reinforcement learning. *Advances in neural information processing systems* 31 (2018).
14. Zahavy, T. et al. A self-tuning actor-critic algorithm. *Advances in neural information processing systems* 33 (2020).
15. Jackson, M. T. et al. Discovering general reinforcement learning algorithms with adversarial environment design. *Advances in neural information processing systems* (2023).
16. Sutton, R. S. & Barto, A. G. *Reinforcement learning: An introduction* (MIT press, 2018).
17. Watkins, C. J. & Dayan, P. Q-learning. *Machine learning* 8, 279-292 (1992).
18. Schulman, J., Wolski, F., Dhariwal, P., Radford, A. & Klimov, O. Proximal policy optimization algorithms. *arXiv preprint arXiv:1707.06347* (2017).
19. Jaderberg, M. et al. Reinforcement learning with unsupervised auxiliary tasks. *arXiv preprint arXiv:1611.05397* (2016).
20. Barreto, A. et al. Successor features for transfer in reinforcement learning. *Advances in neural information processing systems* 30 (2017).
21. Bellemare, M. G., Dabney, W. & Munos, R. A distributional perspective on reinforcement learning. *International conference on machine learning* (2017).

- 324 22. Bellemare, M. G., Naddaf, Y., Veness, J. & Bowling, M. The arcade learning environment: An
325 evaluation platform for general agents. *Journal of artificial intelligence research* 47, 253-279
326 (2013).
- 327 23. Cobbe, K., Hesse, C., Hilton, J. & Schulman, J. Leveraging procedural generation to benchmark
328 reinforcement learning. *International conference on machine learning* (2020).
- 329 24. Hochreiter, S. & Schmidhuber, J. Long short-term memory. *Neural Computation* 9, 1735-1780
330 (1997).
- 331 25. Veeriah, V. et al. Discovery of useful questions as auxiliary tasks. *Advances in neural information*
332 *processing systems* (2019).
- 333 26. Munos, R., Stepleton, T., Harutyunyan, A. & Bellemare, M. Safe and efficient off-policy
334 reinforcement learning. *Advances in neural information processing systems* 29 (2016).
- 335 27. Finn, C., Abbeel, P. & Levine, S. Model-agnostic meta-learning for fast adaptation of deep
336 networks. *International conference on machine learning* (2017).
- 337 28. Mnih, V. et al. Asynchronous methods for deep reinforcement learning. *International conference*
338 *on machine learning* (2016).
- 339 29. Agarwal, R., Schwarzer, M., Castro, P. S., Courville, A. C. & Bellemare, M. Deep reinforcement
340 learning at the edge of the statistical precipice. *Advances in neural information processing systems*
341 34 (2021).
- 342 30. Kapturowski, S. et al. Human-level atari 200x faster. *International conference on learning*
343 *representations* (2023).
- 344 31. Hafner, D. Benchmarking the spectrum of agent capabilities. *International conference on learning*
345 *representations* (2022).
- 346 32. Küttler, H. et al. The netHack learning environment. *Advances in neural information processing*
347 *systems* 33 (2020).
- 348 33. Hambro, E. et al. Insights from the NeurIPS 2021 NetHack challenge. *NeurIPS 2021 Competitions*
349 *and Demonstrations Track* 41-52 (2022).
- 350 34. Espeholt, L. et al. IMPALA: Scalable distributed deep-rl with importance weighted actor-learner
351 architectures. *International conference on machine learning* (2018).
- 352 35. Beattie, C. et al. DeepMind Lab. *arXiv preprint arXiv:1612.03801* (2016).
- 353 36. Racanière, S. et al. Imagination-augmented agents for deep reinforcement learning. *Advances in*
354 *neural information processing systems* 30 (2017).
- 355 37. Schmidhuber, J. *Evolutionary principles in self-referential learning, or on learning how to learn:*
356 *the meta-meta... hook*. Ph.D. thesis, Technische Universität München (1987).
- 357 38. Schmidhuber, J. A possibility for implementing curiosity and boredom in model-building neural
358 controllers. *International conference on simulation of adaptive behavior: From animals to*
359 *animats* (1991).
- 360 39. Schmidhuber, J., Zhao, J. & Wiering, M. Simple principles of metalearning. *Technical report*
361 *IDSIA* 69, 1-23 (1996).
- 362 40. Thrun, S. & Pratt, L. Learning to learn: Introduction and overview, 3-17 (Springer, 1998).
- 363 41. Pan, S. J. & Yang, Q. A survey on transfer learning. *IEEE Transactions on knowledge and data*
364 *engineering* 22, 1345-1359 (2009).
- 365 42. Parisi, G. I., Kemker, R., Part, J. L., Kanan, C. & Wermter, S. Continual lifelong learning with
366 neural networks: A review. *Neural Networks* 113, 54-71 (2019).

- 367 43. Caruana, R. Multitask learning. *Machine learning* 28, 41-75 (1997).
- 368 44. Feurer, M. & Hutter, F. Hyperparameter optimization, 3-33 (Springer, Cham, 2019).
- 369 45. Yao, Q. et al. Taking human out of learning applications: A survey on automated machine
370 learning. *arXiv preprint arXiv:1810.13306* (2018).
- 371 46. Storck, J., Hochreiter, S., Schmidhuber, J. et al. Reinforcement driven information acquisition in
372 non-deterministic environments. *International conference on artificial neural networks* (1995).
- 373 47. Duan, Y. et al. RL 2: Fast reinforcement learning via slow reinforcement learning. *arXiv preprint
374 arXiv:1611.02779* (2016).
- 375 48. Niv, Y., Joel, D., Meilijson, I. & Ruppin, E. Evolution of reinforcement learning in uncertain
376 environments: A simple explanation for complex foraging behaviors (2002).
- 377 49. Xiong, Z., Zintgraf, L., Beck, J., Vuorio, R. & Whiteson, S. On the practical consistency of meta-
378 reinforcement learning algorithms. *Workshop on meta-learning, NeurIPS* (2021).
- 379 50. Sutton, R. S. & Tanner, B. Temporal-difference networks. *Advances in neural information
380 processing systems* (2004).

381

Figure Legends

383 **Figure 1: Discovering a reinforcement learning rule from a population of agents.** **(a) Discovery.**
 384 Multiple agents, interacting with various environments, are trained in parallel according to the learning
 385 rule, defined by the meta-network. In the meantime, the meta-network is optimised to improve the agents'
 386 collective performances. **(b) Agent architecture.** An agent produces the following outputs: 1) a policy
 387 (π), 2) an observation-conditioned prediction vector (y), 3) action-conditioned prediction vectors (z), 4)
 388 action-values (q), and 5) an auxiliary policy prediction (p). The semantics of y and z are determined by
 389 the meta-network. **(c) Meta-network architecture.** A trajectory of the agent's outputs is given as input to
 390 the meta-network, together with rewards and episode termination indicators from the environment
 391 (omitted for simplicity in the figure). Using this information, the meta-network produces targets for all of
 392 the agent's predictions from the current and future timesteps. The agent is updated to minimise the
 393 prediction errors with respect to their targets. **(d) Meta-optimisation.** The meta-parameters of the meta-
 394 network are updated by taking a meta-gradient step calculated from backpropagation through the agent's
 395 update process ($\theta_0 \rightarrow \theta_N$), where the meta-objective to maximise the collective returns of the agents in their
 396 environments.

397 **Figure 2: Evaluation of DiscoRL.** The x-axis represents the number of environment steps in millions.
 398 The y-axis represents the human-normalised interquartile mean (IQM) score for benchmarks consisting of
 399 multiple tasks (Atari, ProcGen, DMLab-30) and average return for the rest. **Disco57** (blue) is discovered
 400 from the Atari benchmark, and **Disco103** (orange) is discovered from Atari, ProcGen, and DMLab-30
 401 benchmarks. The shaded areas show 95% confidence intervals. The dashed lines represent manually-
 402 designed RL rules.

403 **Figure 3: Properties of discovery process.** **(a) Discovery efficiency:** The best DiscoRL was discovered
 404 within 3 simulations of the agent's lifetimes (200 million steps) per game. **(b) Scalability:** DiscoRL
 405 becomes stronger on the ProcGen benchmark as the training set of environments grows. **(c) Ablation:**
 406 The plot shows the performances of variations of DiscoRL on Atari. 'w/o Aux-Pred' is meta-learned
 407 without the auxiliary prediction (p). 'Small Agents' uses a smaller agent network during discovery. 'w/o
 408 Prediction' is meta-learned without learned predictions (y, z). 'w/o Value' is meta-learned without the
 409 value function (q). 'Toy Envs' is meta-learned from 57 grid world tasks instead of Atari games.

410 **Figure 4: Analysis of DiscoRL.** **(a) Behaviour of discovered predictions:** The plot shows how the
 411 agent's discovered prediction (y) changes along with other quantities in *Ms Pacman* (left) and *Breakout*
 412 (right). 'Confidence' is calculated as negative entropy. Spikes in prediction confidence are correlated with
 413 upcoming salient events. For example, they often precede large rewards in *Ms Pacman* and strong action
 414 preferences in *Breakout*. **(b) Gradient analysis:** Each contour shows where each prediction focuses on in
 415 the observation through a gradient analysis in *Beam Rider*. The predictions tend to focus more on enemies
 416 at a distance, whereas the policy and the value tend to focus on nearby enemies and the scoreboard,
 417 respectively. **(c) Prediction analysis:** Future entropy and large-reward events can be better predicted
 418 from discovered predictions. **(d) Bootstrapping horizon:** The plot shows how much the prediction target
 419 produced by DiscoRL changes when the prediction at each timestep is perturbed. The individual curves
 420 correspond to 16 randomly sampled trajectories, while the bold curve corresponds to the average over

421 them. (e) **Reliance on predictions:** The plot shows the performance of the controlled DiscoRL on *Ms*
422 *Pacman* without bootstrapping when updating predictions and without using predictions at all.

423

424 **Methods**

425 **Meta-network**

426 The meta-network maps a trajectory of agent outputs along with relevant quantities from the environment
427 to targets: $m_\eta: f_\theta(s_t), f_{\theta^-}(s_t), a_t, r_t, b_t, \dots, f_\theta(s_{t+n}), f_{\theta^-}(s_{t+n}), a_{t+n}, r_{t+n}, b_{t+n} \mapsto \hat{\pi}, \hat{y}, \hat{z}$ where η
428 represents meta-parameters, and $f_\theta = [\pi_\theta(s), y_\theta(s), z_\theta(s), q_\theta(s)]$ is the agent output with parameters θ . a, r, b are
429 an action taken by the agent, a reward, and an episode termination indicator, respectively. θ^- is an
430 exponential moving average of parameters θ . This functional form allows the meta-network to search over
431 a strictly larger space of rules compared to meta-learning a scalar loss function. This is further discussed
432 in Supplementary Information.

433 The meta-network processes the inputs by unrolling an LSTM backward in time as illustrated in Fig. 1c.
434 This allows it to take into account n-step future information to produce targets, as in multi-step RL
435 methods such as $TD(\lambda)^{51}$. We found that this architecture is computationally more efficient than
436 alternatives such as transformers, while achieving a similar performance as shown in Extended Data Fig.
437 3b.

438 The action-specific inputs and outputs are processed in the meta-network using shared weights over the
439 action dimension, and an intermediate embedding is computed by averaging across it. This allows the
440 meta-network to process any number of actions. More details about it can be found in Supplementary
441 Information.

442 In order to allow the meta-network to discover a wider class of algorithms, such as reward normalisation,
443 that require maintaining statistics over an agent's lifetime, we add an additional recurrent neural network.
444 This 'meta-RNN' is unrolled forward across agent updates (from θ_i to θ_{i+1}), rather than across timesteps in
445 an episode. The core of the meta-RNN is another LSTM module. For each of the agent updates, the whole
446 batch of trajectories is embedded into a single vector which is passed to this LSTM. The meta-RNN can
447 potentially capture the learning dynamics throughout the agent's lifetime, producing targets that are
448 adaptive to the specific agent and the environment. The meta-RNN slightly improved the overall
449 performance as shown in Extended Data Fig. 3a. Further details are described in Supplementary
450 Information.

451 **Meta-optimisation stabilisation**

452 A number of challenges arise when we discover at a large scale, mainly because of unbalanced gradient
453 signals coming from agents in different environments and myopic gradients caused by long lifetimes of
454 agents. We introduce a few methods to alleviate these problems.

455 First, when estimating the advantage term in A2C to estimate $\nabla_\theta J(\theta)$ in the meta-gradient, we normalise
456 the advantage term as follows: $\bar{A} = (A - \mu)/\sigma$, where \bar{A} is a normalised advantage and μ and σ are the
457 exponentially moving average and standard deviation of advantages accumulated over the agent's lifetime.
458 We found that this makes the scale of the advantage term balanced across different environments. In
459 addition, when aggregating the meta-gradient from the population of agents, we take the average of the

460 meta-gradients over all agents after applying a separate Adam optimiser to the meta-gradient calculated
461 from each agent: $\eta \leftarrow \eta + \frac{1}{n} \sum_{i=1}^n ADAM(g_i)$ where g_i is the meta-gradient estimation from the i -th agent
462 in the population. We found that this helps to normalise the magnitude of the meta-gradients from each
463 agent.

464 We add two meta-regularisation losses (L_{ent} and L_{kl}) to the meta-objective $J(\eta)$ as follows: $\square_\epsilon \square_\theta [J(\theta) -$
465 $L_{ent}(\theta) - L_{kl}(\theta)]$. $L_{ent}(\theta) = -\square_{s,a}[H(y_\theta(s)) + H(z_\theta(s,a))]$ is an entropy regularisation of predictions y and z ,
466 where $H(\cdot)$ is the entropy of the given categorical distribution. We found that this helps prevent the
467 predictions from converging prematurely. $L_{kl}(\theta) = D_{KL}(\pi_\theta \| \hat{\pi})$ is the KL divergence between the policy
468 of a target network with an exponential moving average of the agent parameters (θ^-) and the meta-
469 network's policy target ($\hat{\pi}$). This prevents the meta-network from proposing excessively aggressive
470 updates which could lead to collapse.

471 Note that these methods are used only to stabilise meta-optimisation, and they do not determine how the
472 agents are updated. The meta-learned rule still solely determines how the agents are updated.

473 Implementation details

474 We developed a JAX-based framework^{52,53} that distributes computation across TPUs⁵⁴ inspired by the
475 Podracer architectures⁵⁵. In this framework, each agent is simulated independently, with the meta-
476 gradients of all agents being calculated in parallel. The meta-parameters are updated synchronously by
477 aggregating meta-gradients across all agents. We used MixFlow-MG⁵⁶ to minimise the computational cost
478 of the runs.

479 For Disco57, we instantiate 128 agents by cycling through the 57 Atari environments in lexicographic
480 order. For Disco103, we instantiate 206 agents, with two copies of each environment from Atari, ProcGen
481 and DMLab-30. Disco57 was discovered using 1024 TPUv3 cores for 64 hours, and Disco103 was
482 discovered using 2048 TPUv3 cores for 60 hours.

483 The meta-value function used to calculate the meta-gradient is updated using V-Trace³⁴, with a discount
484 factor of 0.997 and a $TD(\lambda)$ coefficient of 0.95. The meta-value function and agent networks are
485 optimised using an Adam optimiser with a learning rate of 0.0003. For meta-parameter updates, we use
486 the Adam optimiser with a learning rate of 0.001 and gradient clipping of 1.0. Each agent is updated
487 based on a batch of 96 trajectories with 29 timesteps each. In each batch, on-policy trajectories and
488 trajectories sampled from the replay buffer are mixed, with replay trajectories accounting for 90% of each
489 batch. At each meta-step, 48 trajectories are generated to calculate the meta-gradient and update the meta-
490 value function.

491 Each agent's parameters are reset after it has consumed its allocated experience budget. When resetting, a
492 new experience budget is sampled from the categories (200M, 100M, 50M, 20M) with a weight inversely
493 proportional to the budget, such that the same amount of total experience is sampled in each category.
494 This was based on our observation that much of learning happens early in the lifetime and demonstrated a
495 marginal improvement in our preliminary small-scale investigation.

496 Hyperparameters and evaluation

497 For evaluation on held-out benchmarks, we only tuned the learning rate from {0.0001, 0.0003, 0.0005}.
498 The rest of the hyperparameters were selected based on baseline algorithms from the literature.

499 The evaluation on Atari games (shown in Fig. 2a and Extended Data Table 1) used a version of the
500 IMPALA³⁴ network with an increased parameter count which matches the agent network size used by
501 MuZero². Specifically, we used a network with four convolutional residual blocks with 256, 384, 384,
502 256 filters, a shared fully-connected final layer of 768 dimensions, and an LSTM-based action-conditional
503 predictions component that is composed of an LSTM with a 1024 hidden state dimension and a 1024
504 dimensional fully-connected layer. DMLab-30 evaluations (Fig. 2c and Extended Data Table 3) use the
505 same action space discretisation and agent network architecture as used in IMPALA. See Extended Data
506 Table 6 for the list of hyperparameters. To verify the statistical significance of our evaluations we used
507 two random seeds for initialisation on each environment from Atari, ProcGen, and DMLab; three seeds on
508 Crafter and Nethack, and five on Sokoban.

509 Analysis details

510 For the prediction analysis in Fig. 4c, we train multiple 3-layer MLPs with 128, 64, and 32 hidden units
511 for each layer respectively. The MLPs are trained to predict quantities such as future entropy and rewards
512 from the outputs of an agent that has been trained on different Atari games using Disco57. We use 10
513 Atari games (Alien, Amidar, Battle Zone, Frostbite, Gravitar, Qbert, Riverraid, Road Runner, Robotank,
514 Zaxxon). The values shown in Fig. 4c are R2 scores for future entropy and test accuracy for large-reward
515 events using 5-fold cross-validation. Extended Data Fig. 2 provides an additional prediction analysis for
516 more quantities. For high-dimensional outputs (y , z , z_a) we used a larger 3-layer MLP with 256 hidden
517 units each.

518 Methods references

- 519 51. Sutton, R. S. Learning to predict by the methods of temporal differences. *Machine Learning* 3, 9-
520 44 (1988). URL <https://api.semanticscholar.org/CorpusID:3349598>.
- 521 52. Bradbury, J. et al. Jax: composable transformations of python+ numpy programs (2018).
- 522 53. DeepMind et al. The DeepMind JAX Ecosystem (2020). URL <http://github.com/google-deepmind>.
- 523 54. Jouppi, N. P. et al. In-datacenter performance analysis of a tensor processing unit. In *Proceedings*
524 *of the 44th annual international symposium on computer architecture*, 1-12 (2017).
- 525 55. Hessel, M. et al. Podracer architectures for scalable reinforcement learning. *arXiv preprint*
526 *arXiv:2104.06272* (2021).
- 527 56. Kemaev, I., Calian, D. A., Zintgraf, L. M., Farquhar, G. & van Hasselt, H. Scalable meta-learning
528 via mixed-mode differentiation. *International conference on machine learning* (2025).

529 Data availability

530 No external data were used for the results presented in the article.

531 Code availability

532 We provide the meta-training and evaluation code, with the meta-parameters of Disco103, under an open
533 source licence at https://github.com/google-deepmind/disco_rl. All of the benchmarks presented in the
534 article are publicly available.

535

536 **End Notes**

537 **Acknowledgements**

538 We thank Sebastian Flennerhag, Zita Marinho, Angelos Filos, Surya Bhupatiraju, Andras György, and
539 Andrei A. Rusu for their feedback and discussions about related ideas. We also thank Blanca Huergo
540 Muñoz, Manuel Kroiss, and Dan Horgan for their help with the engineering infrastructure. Finally, we
541 thank Raia Hadsell, Koray Kavukcuoglu, Nando de Freitas, and Oriol Vinyals for their high-level
542 feedback on the project, and Simon Osindero and Doina Precup for their feedback on the early version of
543 this work.

544 **Author contributions**

545 J.O., I.K., G.F. and D.C. contributed equally; J.O., G.F., I.K., D.C. and L.Z. developed and analysed the
546 method with advice from H.H., S.B. and D.S.; J.O., G.F., M.H., D.C. and I.K. evaluated the method; I.K.
547 led engineering with contributions from J.O., D.C. and G.F; J.O. and G.F. wrote the paper with
548 contributions from L.Z. and D.C.; H.H., S.B. and D.S. advised the team. J.O. and D.S. led the project.

549 **Author information**

550 All authors are affiliated with Google DeepMind, London, UK.

551 Correspondence and requests for materials should be addressed to Junhyuk Oh (junhyuk@google.com) or
552 David Silver (davidsilver@google.com).

553 **Competing interests**

554 A patent application(s) directed to aspects of the work described has been filed and is pending as of the
555 date of manuscript submission. Google LLC has ownership and potential commercial interests in the work
556 described.

557 **Additional information**

558 Reprints and permissions information is available at www.nature.com/reprints.

559 **Supplementary information**

560 Supplementary Information is available for this paper.

561

562 **Extended Data**

563 Extended Data Figure 1: **Robustness of DiscoRL**. The plots show the performance of Disco57 and
564 Muesli on *Ms Pacman* by varying agent settings. 'Discovery' and 'Evaluation' represent the setting used
565 for discovery and evaluation, respectively. (a) Each rule was evaluated on various agent network sizes. (b)
566 Each rule was evaluated on various replay ratios, which define the proportion of replay data in a batch
567 compared to on-policy data. (c) A sweep over optimisers (Adam or RMSProp), learning rates, weight
568 decays, and gradient clipping thresholds was evaluated (36 combinations in total) and ranked according to
569 the final score.

570 Extended Data Figure 2: **Detailed results for the regression and classification analysis**. Each cell
571 represents the test score of one MLP model that has been trained to predict some quantity (columns) given
572 the agent's outputs (rows).

573 Extended Data Figure 3: **Effect of meta-network architecture**. (a) The x-axis represents the number of
574 environment steps in evaluation and the y-axis the IQM on the Atari benchmark. All methods are
575 discovered from 16 randomly selected Atari games. The meta-RNN component slightly improves
576 performance. (b) The x-axis represents the number of environment steps in evaluation and the y-axis the
577 IQM on the Atari benchmark. All methods are discovered from 16 randomly selected Atari games. Each
578 curve corresponds to a different meta-network architecture, with varying number of LSTM hidden units,
579 or its LSTM component is replaced by a transformer. The choice of the meta-net architecture minimally
580 affects performance.

581 Extended Data Figure 4: **Computational cost comparison**. The x-axis represents the amount of TPU
582 hours spent for evaluation. The y-axis represents the performance on the Atari benchmark. Each algorithm
583 was evaluated on 57 Atari games for 200M environment steps. DiscoRL reached MuZero's final
584 performance with approximately 40% less computation.

585 Extended Data Table 1: **Atari57 result**. Each algorithm was evaluated at 200M environment steps. The
586 best result for each game is shown in **bold**.

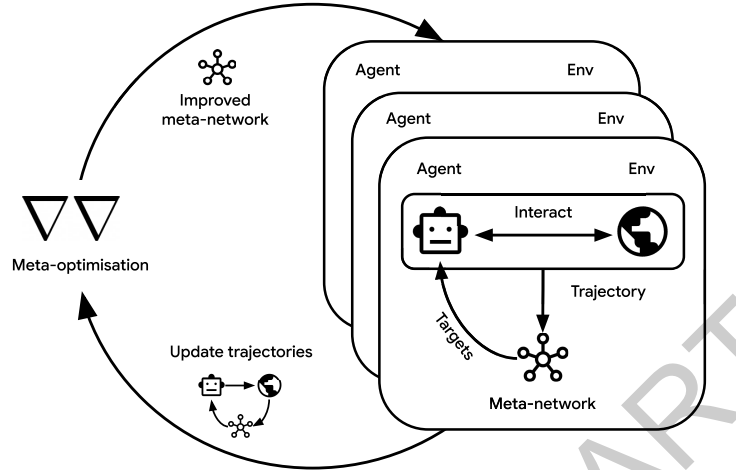
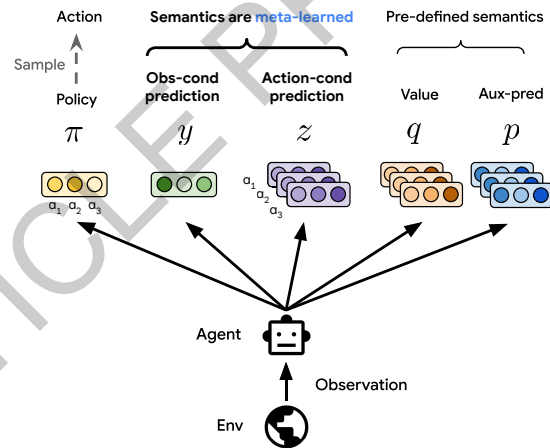
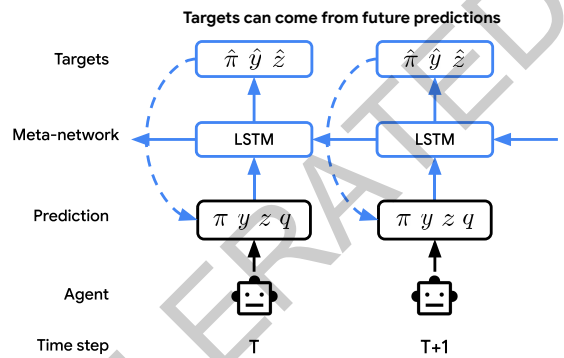
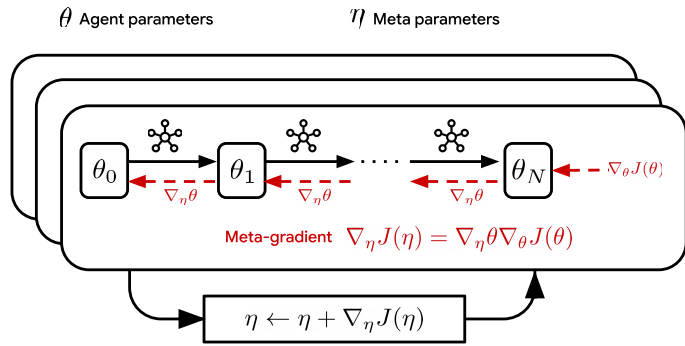
587 Extended Data Table 2: **ProcGen result**. Best result for each game shown in **bold**. The agents were
588 trained and evaluated on 500 training levels.

589 Extended Data Table 3: **DMLab-30 result**. Best result for each task shown in **bold**.

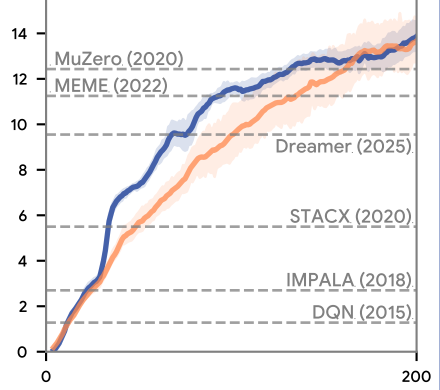
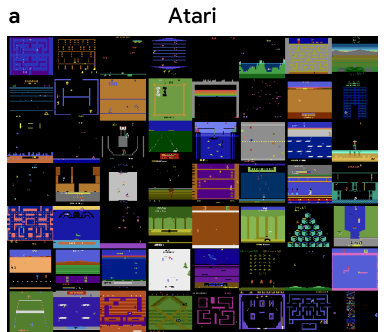
590 Extended Data Table 4: **NetHack result**. Comparison to top 4 submissions from the "Final (Neural)"
591 leaderboard of the NetHack NeurIPS 2021 Challenge³³. Note that median scores were used for ranking
592 submissions on the leaderboard, whereas we report mean scores to be consistent with other benchmarks.

593 Extended Data Table 5: **Crafter result**. Dreamer, Rainbow, PPO, Disco57 @1M and Disco103 @1M all
594 use the same data budget of 1M environment steps, while Disco57 @20M and Disco103 @20M use 20M
595 steps.

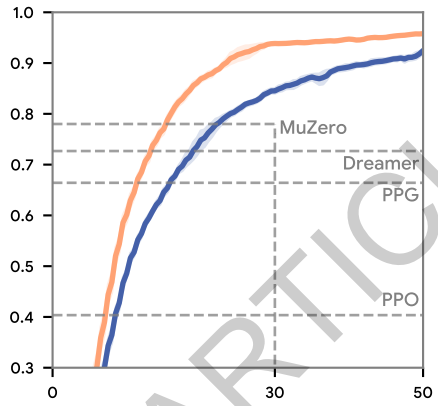
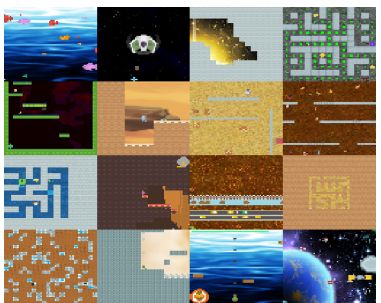
596 Extended Data Table 6: **Hyperparameters of agents in evaluation**.

a Discovery**b Agent****c Meta-network****d Meta-optimisation**

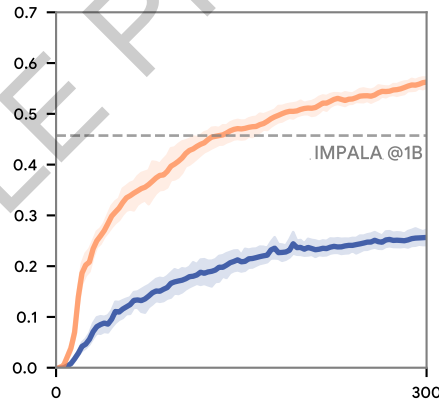
Used to discover Disco57



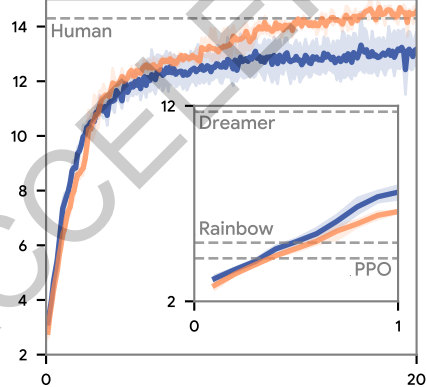
Used to discover Disco103



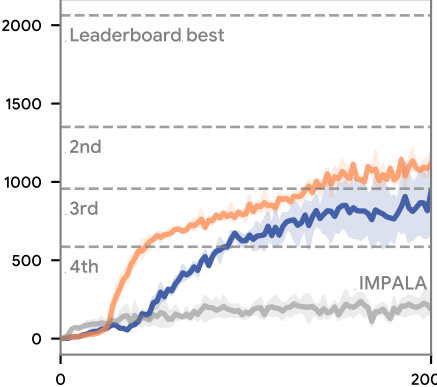
Used to discover Disco103



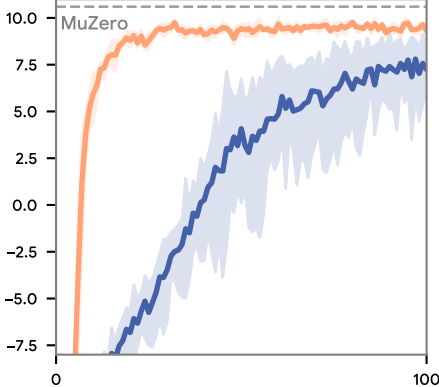
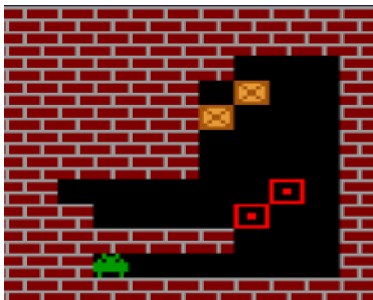
Crafter

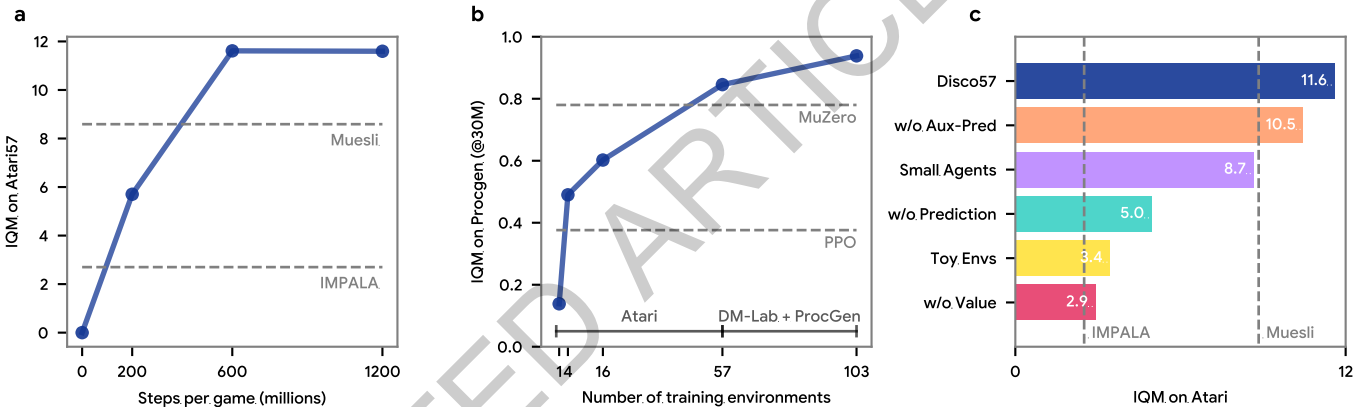


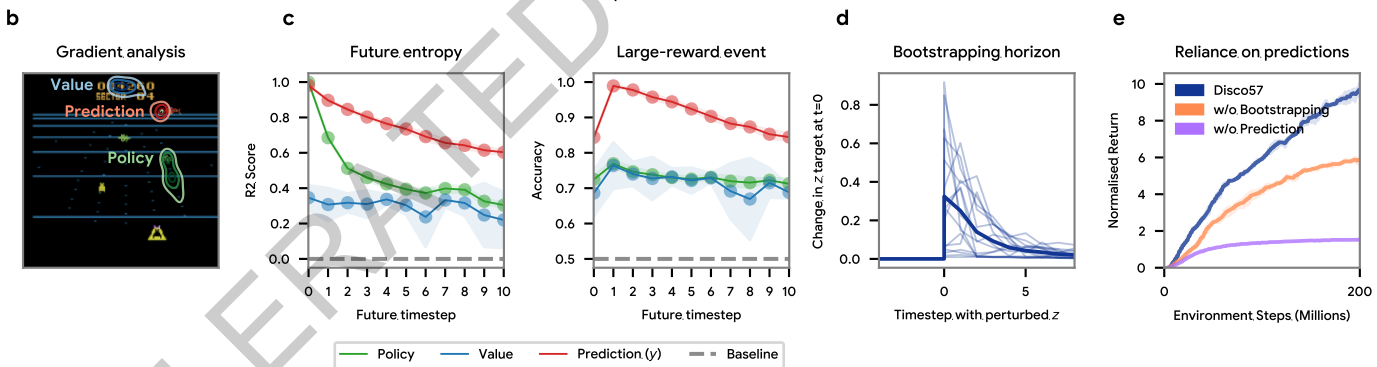
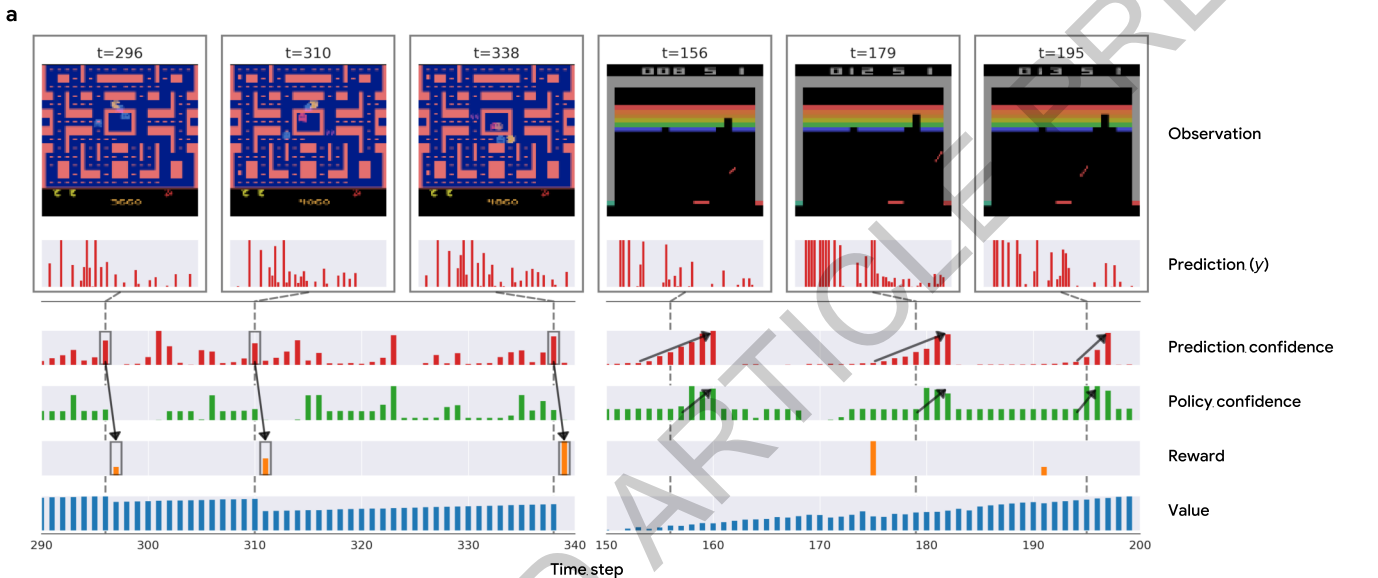
Nethack Challenge

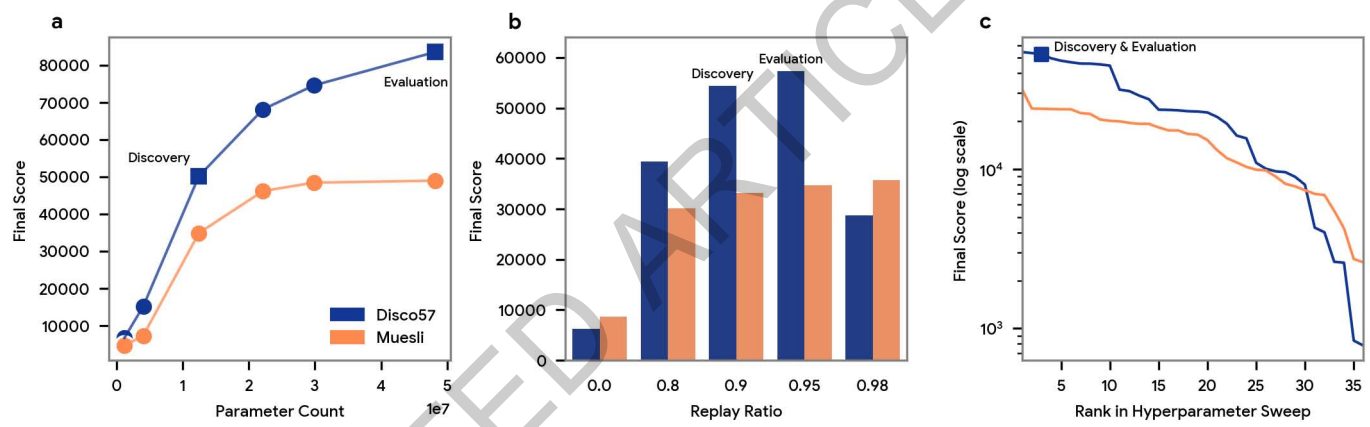


Sokoban





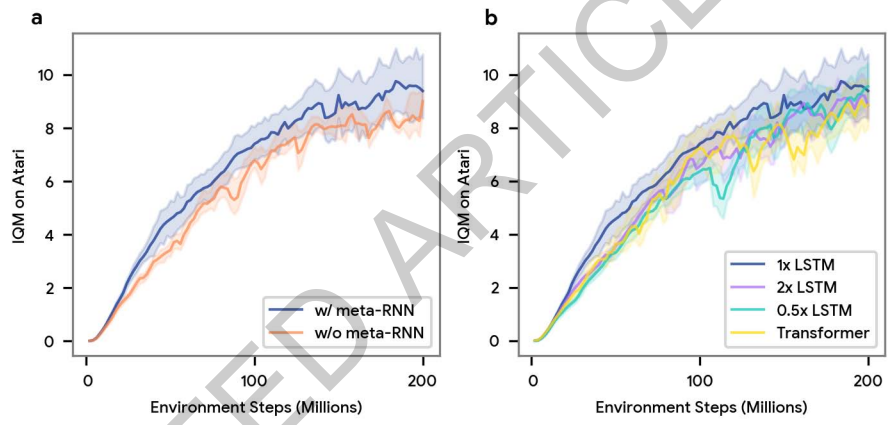




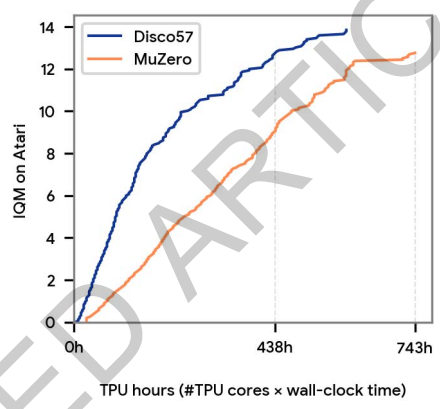
Extended Data Fig. 1

	Targets																															
	π	α	$q(a)$	y	z	advantage	reward	action	entropy	entropy at t+1	entropy at t+5	entropy at t+20	high reward at t+1	high reward at t+5	high reward at t+20	$\ obs_t - obs_{t+1}\ ^2$	$\ obs_t - obs_{t+5}\ ^2$	$\ obs_t - obs_{t+20}\ ^2$	$\ \pi_t - \pi_{t+1}\ ^2$	$\ \pi_t - \pi_{t+5}\ ^2$	$\ \pi_t - \pi_{t+20}\ ^2$	$\ q_t - q_{t+1}\ ^2$	$\ q_t - q_{t+5}\ ^2$	$\ q_t - q_{t+20}\ ^2$	$\ y_t - y_{t+1}\ ^2$	$\ y_t - y_{t+5}\ ^2$	$\ y_t - y_{t+20}\ ^2$	$\ z_t - z_{t+1}\ ^2$	$\ z_t - z_{t+5}\ ^2$	$\ z_t - z_{t+20}\ ^2$		
Features	π	0.77	0.76	0.75	0.93	0.51	0.82	-0	0.11	1	0.73	0.49	0.31	0.29	0.47	0.29	0.54	0.51	0.46	0.54	0.47	0.46	0.38	0.28	0.37	0.65	0.51	0.45	0.58	0.47	0.45	
π	1	0.77	0.76	0.75	0.93	0.51	0.82	-0	0.11	1	0.73	0.49	0.31	0.29	0.47	0.29	0.54	0.51	0.46	0.54	0.47	0.46	0.38	0.28	0.37	0.65	0.51	0.45	0.58	0.47	0.45	
q	-0	0.98	0.97	-0	0.23	-0	-0	-0	-0	0.04	-0	-0	-0	-0	-0.74	-0	-6.1	-0	0.31	0.26	-0	-0.02	-0	-0	-0	-0	-0	-0	-0	-0	-0	
$q(a)$	-0.37	0.95	1	0.38	0.38	0.33	-0	0.01	-0	0.36	0.36	0.19	0.24	-0	-0	0.12	-0	0.5	0.52	0.54	0.11	0.09	0.18	0.12	0.13	0.2	0.28	0.13	0.17	0.1	0.22	0.27
y	-0.84	0.92	0.92	1	0.87	0.77	0.95	0.14	0.08	0.98	0.9	0.73	0.45	0.48	0.93	0.65	0.27	0.7	0.69	0.63	0.76	0.7	0.55	0.55	0.49	0.48	0.89	0.8	0.63	0.8	0.75	0.6
z	-0.97	0.91	0.92	0.93	0.99	0.77	0.95	0.16	0.13	0.96	0.86	0.71	0.42	0.25	0.84	0.49	0.17	0.68	0.68	0.59	0.72	0.67	0.56	0.52	0.49	0.47	0.87	0.78	0.62	0.78	0.72	0.6
$z(a)$	-0.72	0.91	0.93	0.95	0.76	1	0.96	-0	0.08	0.97	0.92	0.72	0.44	0.47	0.93	0.67	0.27	0.68	0.69	0.62	0.79	0.68	0.56	0.57	0.49	0.48	0.9	0.78	0.61	0.82	0.73	0.59

Extended Data Fig. 2



Extended Data Fig. 3



Extended Data Fig. 4

	Random	Human	IMPALA	STACX	Muesli	MuZero	Dreamer	Disco57	Disco103
Alien	228	7128	15962	31809	139409	135541	10977	322137	333105
Amidar	6	1720	1554	3719	21653	1061	3612	1384	14593
Assault	222	742	19148	19648	36963	29697	26010	34676	33546
Asterix	210	8503	300732	245617	316210	918628	441763	814458	773870
Asteroids	719	47389	108590	156096	484609	509953	348684	499430	490463
Atlantis	12850	29028	849967	848007	1363427	1136009	1553222	1112262	1083115
Bank Heist	14	753	1223	1329	1213	14176	1083	1219	1368
Battle Zone	2360	37188	20885	78359	414107	320641	419653	98764	94730
Beam Rider	364	16927	32463	62892	288870	319684	37073	215580	328418
Berzerk	124	2630	1852	1523	44478	19523	10557	74633	72922
Bowling	23	161	59	28	191	156	250	197	219
Boxing	0	12	99	100	99	100	100	99	99
Breakout	2	30	787	717	791	778	384	798	719
Centipede	2091	12017	11049	478347	869751	862737	554553	893158	899572
Chopper Command	811	7388	28255	846788	101289	494578	802698	967905	337167
Crazy Climber	10780	35829	136950	182617	175322	176172	193204	176195	173933
Defender	2874	18689	185203	344453	629482	544320	579875	640052	650392
Demon Attack	152	1971	132826	130741	129544	143846	142109	143656	143710
Double Dunk	-19	-16	0	24	-3	24	24	23	23
Enduro	0	861	0	259	2362	2363	2166	2364	2373
Fishing Derby	-92	-39	44	62	51	69	82	57	76
Freeway	0	30	0	18	33	34	34	33	16
Frostbite	65	4335	317	2522	301694	410173	41888	1652	1214
Gopher	258	2412	66782	87094	104441	121342	87600	125875	120536
Gravitar	173	3351	359	2746	11660	10926	12570	13722	10384
Hero	1027	30826	33730	35559	37161	37249	40677	31605	29031
Ice Hockey	-11	1	3	19	25	40	57	31	40
Jamesbond	29	303	1632	26123	19319	32107	24010	35441	31636
Kangaroo	52	3035	1632	3182	14096	13928	12229	13603	13196
Krull	1598	2666	8147	10480	34221	50137	69858	62579	60703
Kung Fu Master	258	22736	43375	67823	134689	148533	154893	102679	89081
Montezuma Revenge	0	4753	0	0	2359	1450	1852	2559	400
Ms Pacman	307	6952	7342	12647	65278	79319	24079	101876	101290
Name This Game	2292	8049	21537	24616	105043	108133	77809	98867	103914
Phoenix	761	7243	210996	370270	805305	748424	316606	867704	841925
Pitfall	-229	6464	-1	0	0	0	0	-1	0
Pong	-21	15	21	21	20	21	20	20	20
Private Eye	25	69571	98	100	10323	7600	26432	27833	5598
Qbert	164	13455	351200	27264	157353	85926	201084	127630	133099
Riverraid	1338	17118	29608	47671	47323	172266	48080	67916	44260
Road Runner	12	7845	57121	62191	327025	554956	150402	311239	356701
Robotank	2	12	12	61	59	85	132	108	108
Seaquest	68	42055	1753	1744	815970	501236	356584	999994	999991
Skiing	-17098	-4337	-10180	-10504	-18407	-30000	-29965	-29949	-30072
Solaris	1236	12327	2365	2326	3031	4401	5851	2314	2396
Space Invaders	148	1669	43595	34875	59602	31265	15005	64092	44213
Star Gunner	664	10250	200625	298448	214383	158608	408961	568369	564206
Surround	-10	7	7	3	9	10	9	9	8
Tennis	-24	-8	0	19	12	0	-3	23	23
Time Pilot	3568	5229	48481	49932	359105	413988	314947	411305	388002
Tutankham	11	168	292	101	252	318	395	230	347
Up N Down	533	11693	332546	315588	549190	606602	614065	640537	629513
Venture	0	1188	0	0	2104	866	0	1960	0
Video Pinball	0	17668	572898	441220	685436	921563	940631	877143	762964
Wizard Of Wor	564	4757	9157	47854	93291	103463	99136	100942	102435
Yars Revenge	3093	54577	84231	113651	557818	187731	675774	144298	201832
Zaxxon	32	9173	32935	56952	65325	106935	78443	36011	37081

Extended Data Table 1

	Random	Human	PPO	PPG	Dreamer	MuZero	Disco57	Disco103
Steps	-	-	50M	50M	50M	30M	50M	50M
Bigfish	0.00	40.00	10.92	31.26	7.67	30.80	34.61	35.80
Bossfight	0.50	13.00	10.47	11.46	11.16	11.88	12.53	12.65
Caveflyer	2.00	13.40	6.03	10.02	10.78	12.37	9.41	9.93
Chaser	0.50	14.20	4.48	8.57	5.21	4.34	12.83	13.26
Climber	1.00	12.60	7.59	10.24	11.77	9.35	11.74	12.37
Coinrun	5.00	10.00	7.93	8.98	9.87	9.90	9.93	9.95
Dodgeball	1.50	19.00	4.80	10.31	9.36	15.15	18.61	18.72
Fruitbot	-0.50	27.20	20.28	24.32	7.64	8.64	26.41	27.84
Heist	2.00	10.00	2.25	3.77	6.86	3.04	3.53	5.56
Jumper	1.00	10.00	5.09	5.84	9.18	7.75	8.74	9.05
Leaper	1.50	10.00	5.90	8.76	8.34	9.83	9.91	9.89
Maze	4.00	10.00	4.97	7.06	8.93	7.48	9.16	9.52
Miner	1.50	20.00	7.56	9.08	6.07	16.67	18.52	21.48
Ninja	2.00	10.00	6.16	9.38	9.89	9.84	9.88	9.94
Plunder	3.00	30.00	11.16	13.44	24.26	13.26	7.04	7.44
Starpilot	1.50	35.00	17.00	21.57	25.64	41.36	41.42	44.07

Extended Data Table 2

Steps	Random	Human	IMPALA	Disco57	Disco103
Steps	-	-	1000M	300M	300M
Explore Goal Locations Large	3.10	194.50	83.10	36.86	96.62
Explore Goal Locations Small	7.70	267.50	209.40	208.78	224.11
Explore Object Locations Large	4.70	65.70	37.00	32.84	41.78
Explore Object Locations Small	3.60	74.50	57.80	56.08	64.89
Explore Object Rewards Few	2.10	77.70	39.80	30.11	37.99
Explore Object Rewards Many	2.40	106.70	58.70	48.50	55.28
Explore Obstructed Goals Large	2.60	119.50	39.50	5.84	39.46
Explore Obstructed Goals Small	6.80	206.00	135.20	78.18	162.72
Language Answer Quantitative Question	-0.30	184.50	219.40	2.42	318.62
Language Execute Random Task	-5.90	254.10	-49.90	-1.65	310.43
Language Select Described Object	-0.10	389.50	324.60	600.19	605.19
Language Select Located Object	1.90	280.70	189.00	1.27	655.57
Lasertag One Opponent Large	-0.20	12.70	-0.20	-0.01	-0.01
Lasertag One Opponent Small	-0.10	18.60	-0.10	-0.00	-0.05
Lasertag Three Opponents Large	-0.20	18.60	-0.10	0.45	7.27
Lasertag Three Opponents Small	-0.10	31.50	19.10	27.42	34.95
Natlab Fixed Large Map	2.20	36.90	34.70	41.17	55.05
Natlab Varying Map Randomized	7.30	42.40	36.10	37.02	38.97
Natlab Varying Map Regrowth	3.00	24.40	20.70	20.44	25.66
Psychlab Arbitrary Visuomotor Mapping	0.20	58.80	16.40	13.41	16.26
Psychlab Continuous Recognition	0.20	58.30	29.90	30.49	30.35
Psychlab Sequential Comparison	0.10	39.50	0.00	0.00	0.00
Psychlab Visual Search	0.10	78.50	0.00	0.00	0.00
Rooms Collect Good Objects Test	0.10	10.00	9.00	8.61	8.99
Rooms Exploit Deferred Effects Test	8.50	85.70	15.60	39.63	39.45
Rooms Keys Doors Puzzle	4.10	53.80	28.00	26.27	39.45
Rooms Select Nonmatching Object	0.30	65.90	7.30	5.68	6.13
Rooms Watermaze	4.10	54.00	26.90	19.89	31.46
Skymaze Irreversible Path Hard V2	0.10	100.00	13.60	0.00	0.05
Skymaze Irreversible Path Varied V2	14.40	100.00	45.10	43.58	68.17

Extended Data Table 3

	Mean Score
Leaderboard 4th (“Team JustPaulsAI”)	586.06
Leaderboard 3rd (“Team Chaotic-Dwarven”)	956.73
Leaderboard 2nd (“Team KakaoBrain”)	2062.79
Leaderbord Best (“Team RAPH”)	1350.81
IMPALA	188.95
Disco57	938.10
Disco103	1114.24

Extended Data Table 4

Domain	Return
Random	2.10
Human	14.30
PPO	4.20
Rainbow	5.00
Dreamer	11.70
Disco57 @1M	7.58
Disco57 @20M	13.18
Disco103 @1M	6.59
Disco103 @20M	14.56

Extended Data Table 5

	Atari	Crafter	DMLab-30	NetHack	Procgen	Sokoban
Initial learning rate	0.0003	0.0003	0.0005	0.0001	0.0003	0.0003
End learning rate	0.0	0.0003	0	0.0	0.0	0.0
Learning rate schedule	Cosine	Constant	Cosine	Cosine	Cosine	Cosine
Learning rate warmup steps	5×10^6	0	10^6	10^7	10^6	0
Weight decay	0.1	0.3	0.01	0.03	0.1	0.1
Max abs update	1.0	1.0	1.0	0.3	1.0	1.0
Discount factor	0.997	0.997	0.99	0.997	0.997	0.997
Frame stacking	4	32	-	4	4	4
Batch size	96	24	96	96	192	96
TPU cores	16	8	8	16	8	8
Environment steps	2×10^8	5×10^7	10^9	2×10^8	2×10^8	2×10^8
Replay buffer size	1760000	400000	220000	1760000	880000	880000
Replay ratio	0.95	0.99	0.9	0.95	0.9	0.9
Unroll length	29	29	100	29	29	29

Extended Data Table 6